

# LAMINAR FLAMELETS, CONSERVED SCALARS, AND NON-UNITY LEWIS NUMBERS: WHAT DOES THIS HAVE TO DO WITH CHEMISTRY?

J. Houston Miller and Michael A.T. Marro  
Department of Chemistry  
The George Washington University  
Washington, DC 20052

and

Mitchell Smooke  
Department of Mechanical Engineering  
Yale University  
New Haven, CN

**Keywords:** conserved scalar, flamelet, combustion model

## Abstract

In general, computation of laminar flame structure involves the simultaneous solution of the conservation equations for mass, energy, momentum, and chemical species. It has been proposed and confirmed in numerous experiments that flame species concentrations can be considered as functions of a conserved scalar (a quantity such as elemental mass fraction, that has no chemical source term). One such conserved scalar is the mixture fraction which is normalized to be zero in the air stream and one in the fuel stream. This allows the species conservation equations to be rewritten as a function of the mixture fraction (itself a conserved scalar) which significantly simplifies the calculation of flame structure. Despite the widespread acceptance that the conserved scalar description of diffusion flame structure has found in the combustion community, there has been surprisingly little effort expended in the development of a detailed evaluation of how well it actually works. In this presentation we compare the results of a "full" transport and chemical calculation performed by Smooke with the predictions of the conserved scalar approach. Our results show that the conserved scalar approach works because some species' concentrations are *not* dependent only on mixture fraction.

## Introduction

The use of the laminar flamelet concept endures as an important tool in the analysis of turbulent combustion systems. In this technique, the occurrence of flamelet structures is determined probabilistically and then combined with structural information derived from either laminar flame calculations or experiments<sup>1,2,3,4</sup>. A central criticism of the use of these laminar flamelet libraries to model turbulent systems centers on the interaction of small scale turbulent structures with flamelet structures.

In general, computation of laminar flame structure involves the simultaneous solution of the conservation equations for mass, energy, momentum and species. The latter may be solved in the Shvab-Zeldovich form<sup>5</sup> as (Equation 1):

$$L(Y_i) \equiv \rho \frac{\partial Y_i}{\partial t} + \rho V \cdot \nabla Y_i - \nabla \cdot (\rho D_i \nabla Y_i) = w_i$$

where  $Y_i$  is the mass fraction of species  $i$ ,  $w_i$  is the chemical production rate of species  $i$ ,  $\rho$  is the total gas density,  $V$  is the convective velocity, and  $D_i$  is the molecular diffusivity.

Chemical elements (such as  $i = C, H, \text{ or } O$ ) are conserved throughout the chemical reaction mechanism ( $L(Z_i) = 0$ ). Linear combinations of elemental abundances, such as the mixture fraction,  $\xi$ , will also be conserved. Here we adopt Bilger's<sup>6</sup> formulation of mixture fraction in terms of conserved scalars representing relative elemental concentrations for the fuel and oxidant streams in terms of atomic masses for  $C, H$ , and  $O$  and their mass fractions.

It has been previously shown<sup>6</sup> that flame species concentrations are only functions of  $\xi$ . This observation, combined with the assumption of equal diffusivities of all flame species, allows the species conservation equation (Eq. 1) to be rewritten as a function of the mixture fraction. The net chemical production rate for a species then can be written as (Equation 2):

$$w_i = -\left(\frac{1}{2}\right) \cdot \rho \chi \cdot \left(\frac{\partial^2 Y_i}{\partial \xi^2}\right)$$

with the instantaneous scalar dissipation rate,  $\chi$ , defined as (Equation 3):

$$\chi = 2D \cdot (\nabla \xi^2)$$

It has been postulated that concentrations will depend exclusively on mixture fraction when chemical times are short with respect to transport times (i.e., large Damkohler number). It has been shown that this condition is not met for species whose chemistry of formation is slow<sup>7,8</sup>. It has also been suggested that a second independent variable may be required to determine concentrations even for species whose chemistry is fast, and the scalar dissipation rate has been suggested as that variable<sup>9,10,11</sup>. When a species' concentration is determined mostly by its mixture fraction dependence, molecular diffusion will occur preferentially along paths of the steepest mixture fraction gradients in space (Figure 1). We refer to these paths as diffusive trajectories in this paper.

Despite the widespread acceptance that the conserved scalar description of diffusion flame structure has found in the combustion community for the description of turbulent flame structure, there has been surprisingly little effort expended in the development of a detailed evaluation of how well it actually works<sup>12,13</sup>. In this paper we analyze the validity of the conserved scalar approach to the analysis of laminar flame structures. Using the results of a flame structure calculation which has recently been reported<sup>12</sup>, we evaluate the magnitude of the net chemical production rate,  $w_p$ , using Eq. 2 above and compare it to rates calculated from contributions of specific reactions in the flame code. The agreement between these two methods provides a test of the conserved scalar approach.

### Flame Structure Calculations

The chemical structure of an unconfined, co-flowing, axisymmetric  $\text{CH}_4/\text{air}$  diffusion flame was computed with detailed transport and finite rate chemistry. C1 and C2 chemistry were included in a reaction mechanism which involved 83 reversible reactions and 26 species. Details of the calculation have been presented previously, and are summarized briefly below. The fuel was introduced into the flame through an inner tube of radius 0.2 cm and the coflow air through a concentric 5.0 cm diameter outer tube. The results of this flame calculation have been compared with an extensive data base of species concentrations and temperatures collected in a Wolfhard-Parker laminar diffusion flame. Concentration profiles of most flame species agree well for the calculations and the experiments. From calculated species concentrations, temperatures and their positions,  $\xi$  and  $\chi$  can be calculated<sup>12</sup>.

Figure 1 shows contours of mixture fraction in the calculated flame. Also shown are a number of diffusive trajectories through the flame. As stated earlier, these trajectories originate in the fuel rich regions of the flame and follow mixture fraction from rich to lean flame regions along pathways of the steepest gradient of  $\xi$ . As the data in this figure illustrate the mixture fraction gradients along these different vary dramatically, with those which cross the stoichiometric contour near the base of the flame having significantly steeper gradients than those that cross higher in the flame (for example the centerline trajectory).

Figure 2 illustrates the range of mixture fractions and scalar dissipation rates which are observed throughout the computed flame. This data show that at the stoichiometric surface ( $\xi=0.055$ ) the value of the scalar dissipation rate ( $\chi_{ST}$ ) varies dramatically, from nearly 0 up to  $5 \text{ s}^{-1}$ . Extinction occurs in methane/air flames<sup>7</sup> at  $\chi_{ST} = 12 \text{ s}^{-1}$ . Since the data shown in this figure include only locations as low as 0.64 mm above the burner surface, it is reasonable to expect that extinction occurs at lower flame heights.

Figure 3 shows concentrations of methane plotted as a function of mixture fraction for computational nodes throughout the flame. Except for positions very low in the flame, methane concentrations collapse onto a single curve when plotted in this way. Figure 4 shows a similar data presentation for hydrogen atom concentrations. In contrast to the data for methane, the peak shape as well as the peak location shows a dependence on flame location with data low in the flame having larger peak concentrations that occur at lower (leaner) mixture fractions.

### Conserved Scalar Rates

Mass fractions of methane,  $Y_{\text{CH}_4}$ , were calculated and plotted against mixture fraction along each of the chosen trajectories of Figure 1. For these trajectories the dependence of  $Y_{\text{CH}_4}$  on  $\xi$  is largely independent of the trajectory chosen. These curves were numerically differentiated, and combined with local scalar dissipation rates to calculate the net production rate of methane

throughout the flame using Eq. 2. For this calculation we adopt Smooke's formulation for the diffusion coefficient<sup>14</sup>.

Figure 5 shows the results for all except the richest flame regions (for  $\xi > 0.2$ ,  $w$ , rapidly approaches zero). Notice the sharp increase in  $\text{CH}_4$  consumption near the stoichiometric surface. Because the methane concentrations show a common dependence on mixture fraction (Fig. 3), the magnitude of the conserved scalar rates is determined by the magnitude of the scalar dissipation rate which is largest near the base of the flame.

### Chemical Rates

Of the 83 reactions in the mechanism used by Smooke six include methane as a reactant or product. The net rate of methane formation can be evaluated at each location in the flame by summing the contributions of these reactions. Figure 6 shows the dependence of these net rates on mixture fraction along the three diffusive trajectories. As the data in Figs 5 and 6 show, there is good agreement between rates calculated using the conserved scalar approach and that from an evaluation of the rate law. The six reactions that involve methane in the mechanism include its abstraction reaction with hydrogen atoms. The data in Fig. 4 show that hydrogen atom concentrations, like the scalar dissipation rate, show a strong dependence on flame position with larger concentrations low in the flame.

Net chemical production rates for hydrogen atoms using the conserved scalar approach do not agree with those calculated using the hydrogen rate law in the mechanism. This result might have been anticipated given the non-collapse of the concentration versus mixture fraction data shown in Fig. 4.

### Conclusions

In this paper we have compared the results of a "full" transport and chemical calculation performed by Smooke with the predictions of the conserved scalar approach. Our results show that the conserved scalar approach works because some species' concentrations are *not* dependent only on mixture fraction. For the latter species, the net chemical rates can not be evaluated from conserved scalar expressions. The current effort in this project focuses on the cause for the hydrogen atom concentration dependence on flame location. One possibility for this relationship is the fast diffusion velocity that exists for hydrogen atoms near the base of the flame because of its steep concentration gradients. For this species, transport times are short and of the same magnitude as chemical times. It is interesting to conjecture that this fast transport may be cast quantitatively as a dependence of concentration on scalar dissipation rates as has been proposed for flamelet modeling of turbulent combustion.

### References

1. Williams, F.A. *Turbulent Mixing in Non-Reactive and Reactive Flow*; Plenum: New York, 1975, 198.
2. Peters, N. *Twenty-First Symposium (International) on Combustion*; The Combustion Institute: Pittsburgh, 1986, 1231.
3. Bilger, R.W. *Twenty-Second Symposium (International) on Combustion*; The Combustion Institute: Pittsburgh, 1988, 475.
4. Hermanson, J.C.; Vranos, A. *Combust. Sci. and Tech.*; 1991, 75, 339.
5. Williams, F.A. *Combustion Theory*; Addison-Wesley: Reading, MA, 1965.
6. Bilger, R.W. *Combust. and Flame*; 1977, 30, 277.
7. Smyth, K.C.; Taylor, P.H. *Chem. Phys. Lett.*; 1985, 122, 518.
8. Miller, J.H. *Twenty-Fourth Symposium (International) on Combustion*; The Combustion Institute: Pittsburgh, 1992, 131.
9. Drake, M.C. *Twenty-First Symposium (International) on Combustion*; The Combustion Institute: Pittsburgh, 1986, 1579.
10. Seshadri, K.; Maub, F.; Peters, N.; Warnatz, J. *Twenty-Third Symposium (International) on Combustion*; The Combustion Institute: Pittsburgh, 1990, 559.
11. Peters, N.; Kee, R.J. *Combust. and Flame*; 1987, 68, 17.
12. Norton, T.S.; Smyth, K.C.; Miller, J.H.; Smooke, M.D. *Combust. Sci. and Tech.*; 1993, 90, 1.
13. Smooke, M.D.; Lin, P.; Lam, J.K.; Long, M.B. *Twenty-Third Symposium (International) on Combustion*; The Combustion Institute: Pittsburgh, 1990, 575.
14. Smooke, M.D.; Giovangigli, V. *Reduced Kinetic Mechanisms and Asymptotic Approximations for Methane-Air Flames*; Lecture Notes in Physics, Springer-Verlag: Berlin, 1991, 384, 1.

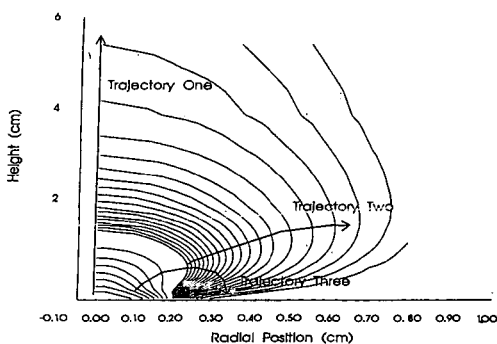


Figure One: Pictorial representation of the diffusive trajectories chosen across contours of mixture fraction,  $\xi$ .

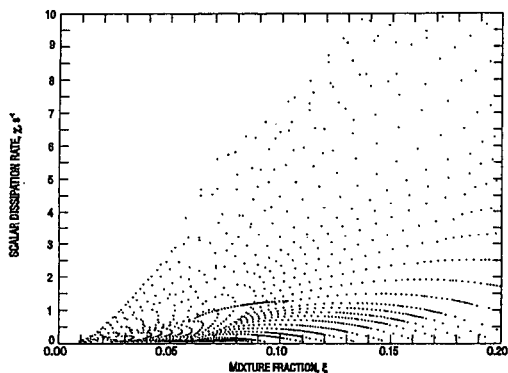


Figure Two: Plot of scalar dissipation rate,  $\chi$ , versus mixture fraction,  $\xi$ . Values move from low to high in the flame from top to bottom.

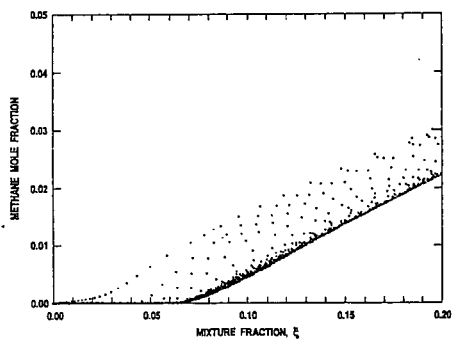


Figure Three: Plot of  $\text{CH}_4$  mole fraction versus mixture fraction,  $\xi$ . (Positions low in the flame are on the left).

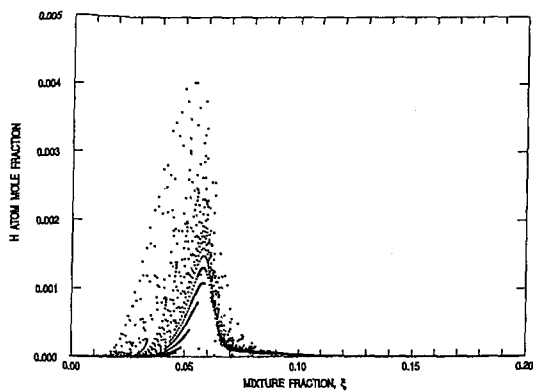


Figure Four: Plot of H atom mole fraction versus mixture fraction,  $\xi$ . (Values move from low to high in the flame from top to bottom).

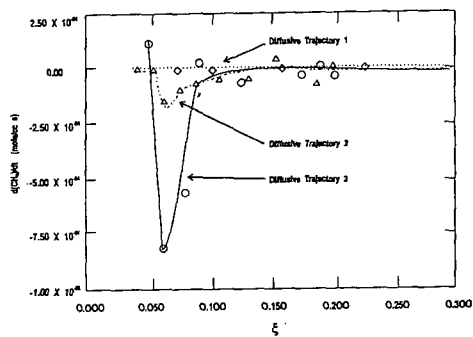


Figure Five: Conserved Scalar predicted rates of  $\text{CH}_4$  production versus mixture fraction,  $\xi$ , along the diffusive trajectories chosen.

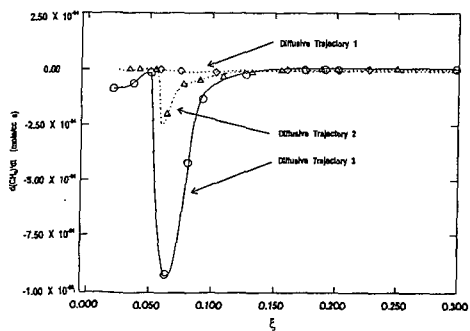


Figure Six: Chemical rate of  $\text{CH}_4$  formation versus mixture fraction,  $\xi$ , along the chosen diffusive trajectories.